ELSEVIER

Mathematics and Computers in Simulation 61 (2003) 209–218

MATHEMATICS AND COMPUTERS IN SIMULATION

www.elsevier.com/locate/matcom

Finite element simulation of thermoforming processes for polymer sheets

M.K. Warby [a], J.R. Whiteman [a,*], W.-G. Jiang [a], P. Warwick [b], T. Wright [b]

[a] *Department of Mathematical Sciences, Institute of Computational Mathematics BICOM, Brunel University, Uxbridge, Middlesex UB8 3PH, UK*

[b] *Autotype International Ltd., Grove Road, Wantage, OX12 7BZ, UK*

Abstract

The problem of modelling and the finite element simulation of thermoforming processes for polymeric sheets at various temperatures and for different loading regimes is addressed. In particular, the vacuum forming process for sheets at temperatures of approximately 200 °C and the Niebling process for sheets at temperature of 100 °C with high pressure loading are both described. Discussion is given to the assumptions made concerning the behaviour of the polymers and the physical happenings in the process in order that realistic models of the inflation part of each process may be produced. Stress–strain curves produced from experimental testing of BAYFOL® at various strain rates and temperatures are presented. A model for the elastic–plastic deformation of BAYFOL® is described and is used within the finite element framework to simulate the inflation part of the Niebling process. Numerical results for the deformation of sheets into a mould in the Niebling context are presented.

Keywords: Finite element simulation; Thermoforming process; Polymeric sheets

1. Introduction and description of the processes

This paper is concerned with the computational modelling of thermoforming processes for polymeric sheets. These are processes in which the thin hot solid sheets, clamped at their edges, are subjected to pressures so that they undergo large deformation into moulds to become thin walled structures, as for example in Fig. 1.

The complete thermoforming process may be described in the terms of the following sequence of phases:

(a) the sheet, clamped at its edges (see Fig. 2) is heated. Due to the increase in temperature the sheet expands, becomes less rigid, and may sag under gravity;

* Corresponding author. Tel.: 44-1-895-203270; fax: 44-1-895-203303.
E-mail address: john.whiteman@brunel.ac.uk (J.R. Whiteman).

0378-4754/02/$ – see front matter
PII: S0378-4754(02)00077-0

Fig. 1. Typical product produced by pressure thermoforming.

(b) the heaters are removed;
(c) the pressure is immediately applied (either to the upper face of the sheet (pressure assisted thermoforming) or by evacuation of the volume between the sheet and the mould (vacuum forming)), deformation takes place so that the hot sheet comes into contact with the mould which is cooler (effectively freezing the sheet) and takes up the mould shape;
(d) the pressure is maintained, whilst the thin walled structure cools, it has been observed that at this stage the structure remains in contact with the mould;
(e) the pressure is removed, it is thought that at this stage the structure also remains in contact with the mould;
(f) the structure is blown off the mould, possibly changing shape due to springback, and takes up its final equilibrium shape.

In recent years, much work has been done on the computational simulation of thermoforming processes, concentrating almost exclusively on modelling the deformation which takes place in phase (c), see e.g. [3–5,9,12,14,15]. The deformation and final thickness of the structure are the quantities of prime interest

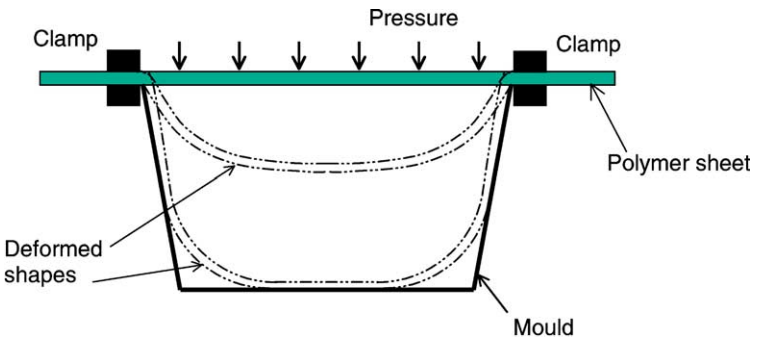

Fig. 2. Schematic diagram of pressure thermoforming process.

and it is assumed that the majority of the deformation and change in thickness of the sheet take place in phase (c). It is also the numerical simulation of the inflation phase (c) that will be our primary interest in this paper. Thus, where the effectiveness of a numerical simulation is discussed, it is the numerical results obtained from modelling (c) that are compared with the final shapes and thicknesses of thermoformed structures obtained experimentally and which of course contain all the physical effects of the phases (a)–(f).

In the present work, we are concerned with the simulation of the phase (c) of the thermoforming process in the two contexts: the vacuum forming process that takes place with the sheet at a temperature of 180–200 °C, and the process in which the deformation takes place under much higher pressure (typically 120 bar), but at much lower sheet temperatures (∼100 °C), the so-called *Niebling process*.

We are, in general, seeking models that simulate a range of thermoforming processes effectively, and for this we have to make a number of seminal assumptions. The two major ones of these are:

- the deformation process is quasi-static,
- the sheets stick to the moulds on contact.

In this paper, we shall primarily be concerned with the Niebling process for BAYFOL® (a blend of bisphenol-A-polycarbonate and polybutylene-terephthalate) and will produce computational simulations of phase (c) of this process.

Experimental test results (see Section 2) for BAYFOL® suggest that it is reasonable in this case to make the additional assumption:

- the deformation in phase (c) is elastic–plastic.

The elastic–plastic model of the large deformation/strain inflation phase is described in Section 3. The primary unknowns in the model at each stage are the displacements u at points throughout the sheet for each specific applied pressure. The finite element discretisation of the model produces numerical approximations to these displacements, which enable paths of the deformation of points in the sheet with increasing pressure, as well as wall thicknesses in the thermoforming structures, to be obtained. Details of the numerical results are discussed in Section 4.

2. Some test results for BAYFOL®

A series of uniaxial constant strain rate tests for BAYFOL® has been performed under controlled isothermal conditions, with temperatures ranging from 100 to 200 °C and with strain rates ranging from 0.02 to 1.00 s^{-1}. It has been found that at 100 °C, a temperature appropriate to the Niebling process, the stress–strain curves are not sensitive to the rates at which the strains are applied. For the range of strain rates as earlier, at 100 °C all our tests produce curves of true stress against true strain close to that given in Fig. 3. This feature is not found for BAYFOL® at higher temperatures, as can be seen from Fig. 4, where the curves arising from tests at different strain rates at 200 °C are given.

The form of the curve in Fig. 3 indicates that at 100 °C, during the inflation phase (c), the BAYFOL® sheet deforms in an elastic–plastic manner. In our simulation of the inflation part of the Niebling process, we have, therefore, chosen a rate independent elastic–plastic model, with associative plasticity and isotropic hardening, to represent the material behaviour at the fixed temperature of 100 °C. In the post-yield state the curve

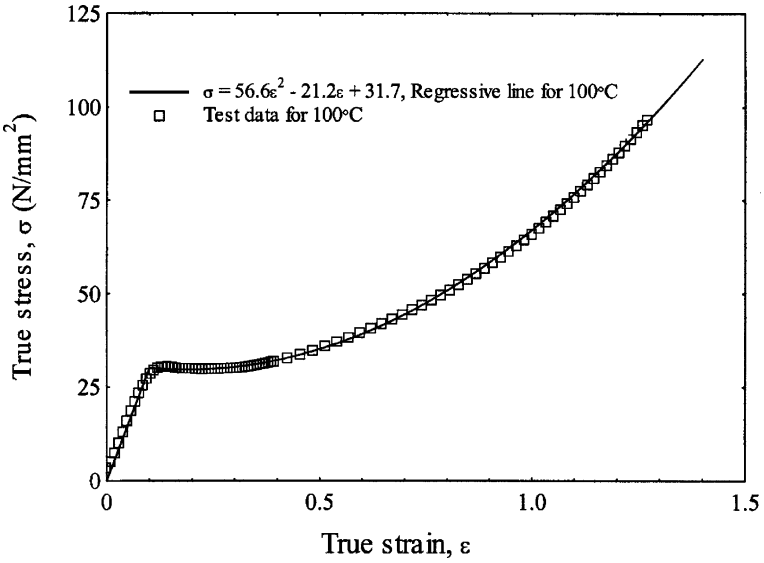

Fig. 3. Variation of true stress with true strain at temperatures of 100 °C.

$$\sigma = 56.6\varepsilon^2 - 21.2\varepsilon + 31.7,$$

where σ and ε are respectively, the true stress and true strain, is the best least squares quadratic fit to the experimental data, and has been used throughout our algorithm.

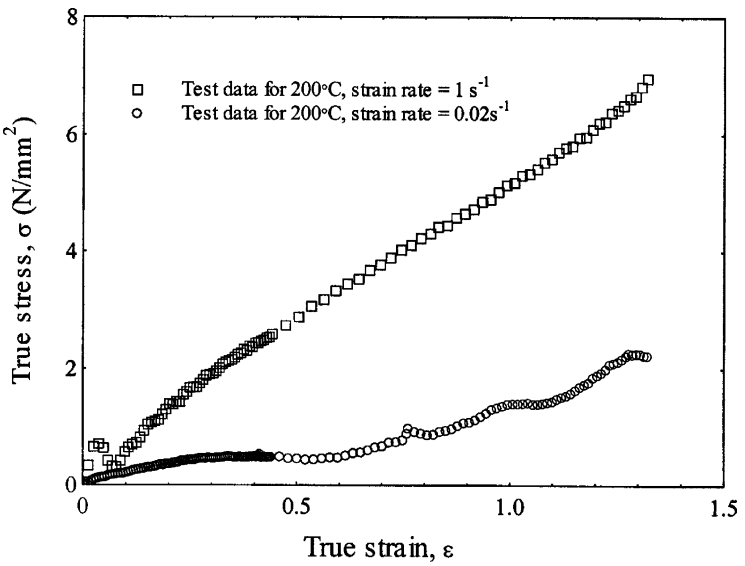

Fig. 4. Variation of true stress with true strain at temperature of 200 °C.

3. Large strain elastic–plastic updated Lagrangian model

In modelling, the inflation phase (c) for BAYFOL® in the Niebling context we assume that the sheet undergoes (rate-independent) finite, geometrically nonlinear, deformation pre- and post-yield.

Many of the details of this finite deformation model resemble those of standard models which were given for the case when strains are infinitesimal by Owen and Hinton [10], Hlavacek et al. [7], Kuczma and Whiteman [8], Simo and Taylor [11], and were developed further for the finite strain case using a logarithmic strain measure, as for example, in Zienkiewicz and Taylor [16], Bathe [2], and Bathe and Eterovic [6]. In order to treat the plastic deformation the model contains a yield criterion and, post-yield, there is a flow rule and the material undergoes work hardening. The model follows closely that given by Weber et al. [13], and due to the discretisation of the flow rule involves an incremental procedure.

In its undeformed state, the sheet occupies the domain $\Omega \in \Re^3$. In the deformation, a point $\underline{x} \equiv (x_1, x_2, x_3) \in \Omega$ moves to $\underline{x} + \underline{u}(\underline{x})$, where $\underline{u} \equiv (u_1, u_2, u_3)^{\mathrm{T}}$ is the displacement vector. The deformation gradient tensor $\underline{\underline{F}}$ is defined as

$$\underline{\underline{F}} \equiv \underline{\underline{I}} + \nabla \underline{u} = \underline{\underline{I}} + \left(\frac{\partial u_i}{\partial x_j} \right), \tag{1}$$

$i, j = 1, 2, 3$, and has the polar decomposition

$$\underline{\underline{F}} = \underline{\underline{R}}\,\underline{\underline{U}}, \tag{2}$$

where $\underline{\underline{R}}$ is the (orthogonal) rotation tensor and $\underline{\underline{U}}$ the (symmetric positive definite) right stretch tensor. The tensor $\underline{\underline{U}}$ admits a spectral decomposition in terms of its eigenvalues, $\lambda_1,\ \lambda_2,\ \lambda_3$, which are the principle stretch ratios, and the orthonomal eigenvectors $\underline{v}_1,\ \underline{v}_2,\ \underline{v}_3$ of $\underline{\underline{U}}$, which are the principle directions of $\underline{\underline{U}}$, such that

$$\underline{\underline{U}} = \sum_{i=1}^{3} \lambda_i \underline{v}_i . \underline{v}_i^{\mathrm{T}}. \tag{3}$$

The logarithmic strain tensor $\underline{\underline{E}}$ is defined as

$$\underline{\underline{E}} = \sum_{i=1}^{3} (\ln(\lambda_i)) \underline{v}_i . \underline{v}_i^{\mathrm{T}}. \tag{4}$$

In each increment the sheet must be in equilibrium under the applied load and constraint conditions. In the $(n+1)$th load step, we require to find the increment of displacement ${}^{(n+1)}\Delta\underline{u}$ arising from the increment of load and, assuming that the displacement ${}^{(n)}\underline{u}$, the stress tensor ${}^{(n)}\underline{\underline{\sigma}}$ and the yield stress ${}^{(n)}\sigma_y$ are known from the previous load step, we can then calculate ${}^{(n+1)}\underline{u}$ from ${}^{(n+1)}\underline{u} = {}^{(n)}\underline{u} + {}^{(n+1)}\Delta\underline{u}$.

Thus, at each load step we solve a weak form of the equilibrium equation

$$\int_{{}^{(n)}\Omega} {}^{(n+1)}S_{ij}({}^{(n+1)}\Delta\underline{u}, {}^{(n)}\underline{u})\zeta_{ij}(\underline{v}) = G(\underline{v}), \tag{5}$$

where ${}^{(n+1)}\Delta\underline{u}$ is the primary unknown, the relative first Piola-stress ${}^{(n+1)}S_{ij}$ is defined in terms of the true stress ${}^{(n+1)}\sigma_{ij}$ by

$${}^{(n+1)}\underline{\underline{S}} \equiv \det({}^{(n+1)}\Delta\underline{\underline{F}})({}^{(n+1)}\underline{\underline{\sigma}})({}^{(n+1)}\Delta\underline{\underline{F}})^{-\mathrm{T}}, \tag{6}$$

$(n+1)$ denotes the load step, $\zeta_{ij}(\mathfrak{v})$ is the usual infinitesimal strain tensor operator acting on the test vector $\mathfrak{v}$ and the G depends on the loading of the problem during the step.

In order to close the problem, we need a constitutive relation for the material in the load step. In each load step, the system of nonlinear equations arising from Eq. (5) will be solved iteratively using a Newton–Raphson procedure, and once the iteration has converged the load is incremented.

We, thus, get the displacement field for successively larger and larger loads. For the $(n+1)$th step we assume that we know initially ${}^{(n)}\mathfrak{u}$, ${}^{(n)}\underline{\sigma}$, ${}^{(n)}\underline{E}$, ${}^{(n)}\sigma_y$.

In order to define the procedure in the step we work in terms of "trial-quantities" denoted by subscript $(*)$. For a trial increment of displacement ${}^{(n+1)}\Delta\mathfrak{u}_*$ in the load step we have the trial relative deformation gradient

$$ {}^{(n+1)}\Delta\underline{E}_* = {}^{(n+1)}\underline{E}_*({}^{(n)}\underline{E})^{-1} \tag{7} $$

which has polar decomposition

$$ {}^{(n+1)}\Delta\underline{E}_* = {}^{(n+1)}\Delta\underline{R}_*\,{}^{(n+1)}\Delta\underline{U}_*, \tag{8} $$

and we define the trial increment of logarithmic strain

$$ {}^{(n+1)}\Delta\underline{E}_* \equiv \ln({}^{(n+1)}\Delta\underline{U}_*). \tag{9} $$

The corresponding trial deviatoric stress increment is

$$ {}^{(n+1)}\Delta\underline{T}'_* \equiv 2\mu\,{}^{(n+1)}\Delta\underline{E}'_*, \tag{10} $$

where μ is the shear modulus of the material and ${}^{(n+1)}\Delta\underline{E}'_*$ is the trial incremental deviatoric logarithmic strain. Defining the mean trial stress increment as

$$ {}^{(n+1)}\Delta\underline{T}^{\mathrm{m}}_* \equiv \tfrac{1}{3}\mathrm{tr}\left({}^{(n+1)}\Delta\underline{T}_*\right) = 3\kappa\,{}^{(n+1)}\Delta\underline{E}^{\mathrm{m}}_*, \tag{11} $$

where κ is the bulk modulus of the material and ${}^{(n+1)}\Delta\underline{E}^{\mathrm{m}}_*$ is the mean trial incremental logarithmic strain, and the stress measure

$$ {}^{(n+1)}\underline{T}_* \equiv ({}^{(n+1)}\Delta\underline{R}_*)^{\mathrm{T}}({}^{(n+1)}\underline{\sigma})({}^{(n+1)}\Delta\underline{R}_*), \tag{12} $$

the total stress resulting from the load increment is

$$ {}^{(n+1)}\underline{T}_* = {}^{(n)}\underline{T} + 2\mu\,{}^{(n+1)}\Delta\underline{E}'_* + 3\kappa\,{}^{(n+1)}\Delta\underline{E}^{\mathrm{m}}_*. \tag{13} $$

In order to test for the onset of plastic deformation, we now need a yield criterion, equivalent trial tensile stress, which is defined by

$$ {}^{(n+1)}\bar{\sigma}_* \equiv \sqrt{\tfrac{3}{2}\,{}^{(n+1)}\underline{T}'_* \cdot {}^{(n+1)}\underline{T}'_*}, \tag{14} $$

and with this we test whether

$$ {}^{(n+1)}\bar{\sigma}_* \le {}^{(n)}\sigma_y;\ \text{(von Mises yield criterion)}, \tag{15} $$

If ${}^{(n+1)}\bar{\sigma}_* \le {}^{(n)}\sigma_y$, then the deformation is elastic, whereas if ${}^{(n+1)}\bar{\sigma}_* > {}^{(n)}\sigma_y$ we need to allow for the onset of the plasticity. In this case, we calculate the corrected trial equivalent tensile stress ${}^{(n+1)}\tilde{\bar{\sigma}}_*$ from the hardening rule

$$ {}^{(n+1)}\tilde{\bar{\sigma}}_* \equiv {}^{(n+1)}\sigma_y = {}^{(n)}\sigma_y + h\,{}^{(n+1)}\Delta E^P_*, \tag{16} $$

where $h = h({}^{(n+1)}\sigma_y)$ is the slope function of the hardening curve (derived from material tensile testing), and ${}^{(n+1)}\Delta E^P_*$ is the trial plastic strain increment.

There is also the flow rule in which

$$ {}^{(n+1)}\tilde{\bar{\sigma}}_* = {}^{(n+1)}\bar{\sigma}_* - 3\mu\,{}^{(n+1)}\Delta E^P_*; \text{ (Prandtl Reuss)}. \tag{17} $$

Eqs. (16) and (17) can be solved to produce ${}^{(n+1)}\tilde{\bar{\sigma}}_*$, the equivalent tensile stress, by definition ${}^{(n+1)}\sigma_y = {}^{(n+1)}\tilde{\bar{\sigma}}_*$, and the stress measure $\underline{\underline{T}}_*$ can be updated from

$$ {}^{(n+1)}\underline{\underline{T}}_* = \left(\frac{{}^{(n+1)}\tilde{\bar{\sigma}}_*}{{}^{(n+1)}\bar{\sigma}_*}\right) {}^{(n+1)}\underline{\underline{T}}'_* + \frac{1}{3}\mathrm{tr}({}^{(n+1)}\underline{\underline{T}}_*)\underline{\underline{I}} \tag{18} $$

The trial true stress ${}^{(n+1)}\underline{\underline{\sigma}}_*$ is then obtained from

$$ {}^{(n+1)}\underline{\underline{\sigma}}_* = {}^{(n+1)}\Delta\underline{\underline{R}}\,{}^{(n+1)}\underline{\underline{T}}_*\,({}^{(n+1)}\Delta\underline{\underline{R}})^{\mathrm{T}}. \tag{19} $$

Substitution of Eq. (19) in Eq. (6) gives an expression for the Piola-stress, which can be substituted in Eq. (5) finally to close the procedure.

4. Finite element implementation

The large deformation elastic–plastic model has been described in terms of trial quantities. In the implementation, we discretise in space by the finite element method in the usual way and the trial quantities at each load level are increments of the nodal displacements which are determined by a Newton–Raphson iterative procedure in order to satisfy the nonlinear equations which result from the equilibrium Eq. (5).

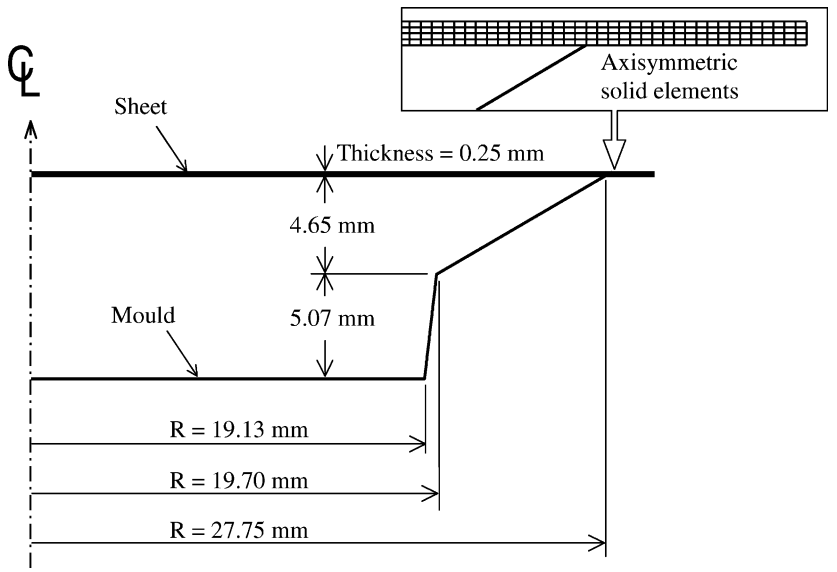

Fig. 5. Axisymmetric finite element model of the thermoforming process.

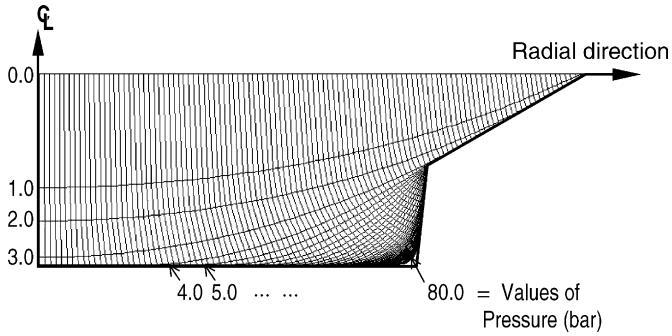

Fig. 6. Sequential deformed shapes and material paths for inflation stage, temperature 100 °C.

In order to deal with the volumetric locking problem which can occur in this context, mean dilatation technique is employed [2].

In the present work, the procedure is applied to model the deformation of the sheet into an axisymmetric mould. This enables a two-dimensional problem with geometry as in Fig. 5 to be treated. In the finite element discretisation, a uniform mesh with four layers of four node isoparametric rectangular elements through the thickness is put over the sheet section, giving a total of 960 elements. Deformation paths for points on the bottom surface of the sheet together with sheet deformation profiles for different pressure levels during the inflation process are given in Fig. 6. It can be seen that high pressure levels are required to force the sheet into the acute corner of the mould. Thickness profiles of the deformed sheet in this axisymmetric case are given in Fig. 7 for pressures corresponding to those in Fig. 6. As might be expected the deformed sheet is thinnest in the neighbourhood of the acute mould corner.

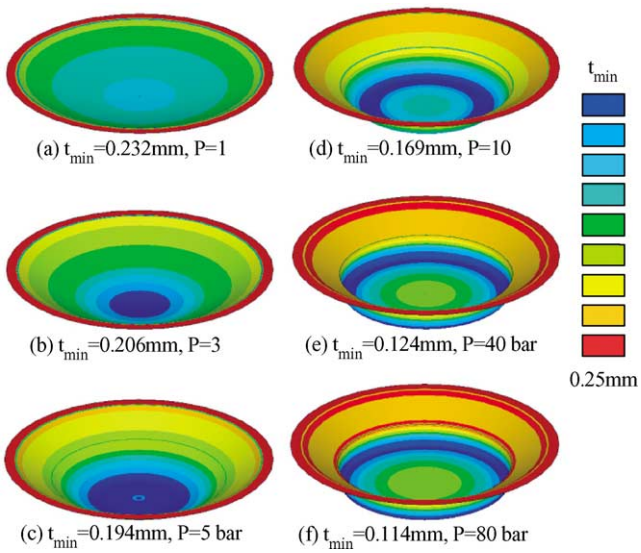

Fig. 7. Thickness distribution on deformed shapes, temperature 100 °C, with various pressures.

5. Conclusion

It can be seen from the results of this paper that the Niebling process for BAYFOL® can be modelled effectively using an elastic–plastic model and its finite element discretisation. As was said earlier the motivation for using the elastic–plastic model comes from the test results which are presented in Fig. 3. The results arising from the model do indicate that it could be used in a predicative manner for modelling Niebling processes and clearly the next step in the project which is involving this work will be to make a comparison between numerical results and results which come from actual practical processes in the industrial context.

In Section 1, we discussed the thermoforming process for temperatures around 200 °C. The test results for BAYFOL® sheets at this temperature indicate that the material behaviour is no longer strain rate independent; in fact, it is highly strain rate dependent. Thus, in order to be able to model the inflation phase of the thermoforming process, it is likely that rate dependent effects will need to be included in the model in order to get an accurate simulation of the process.

Clearly, the work of this paper has been concentrated on phase (c) of the complete thermoforming process under the assumption that the sheet sticks to the mould on contact. It is necessary that further investigation should take place to determine whether this total sticking condition is appropriate or whether some more sophisticated friction-based contact condition should be included in the model.

In order to have a complete model of thermoforming processes for polymer sheets it is obvious that phases (a) and (d)–(f) of the process will need to be modelled. It is not clear at the moment which of these has the greatest importance in the overall production of polymeric structures once phase (c) has been modelled effectively. Further development is also necessary for the more theoretical aspects of this type of constrained sheet deformation. As a starting point we refer the reader to Andrä et al. [1] who modelled the sheet under the simplified assumptions that it is a hyperelastic membrane and that the contact condition is that of perfect sticking.

References

[1] H. Andrä, M.K. Warby, J.R. Whiteman, Contact problems of hyperelastic membranes: existence theory, Math. Meth. Appl. Sci. 23 (2000) 865–895.
[2] K.-J. Bathe, Finite Element Procedures, Prentice-Hall, New Jersey, 1999.
[3] H.G. deLorenzi, H.F. Nied, Blow moulding and thermoforming of plastics: finite element modeling, Comp. Struct. 26 (1987) 197–206.
[4] H.G. deLorenzi, H.F. Nied, Finite element simulation of thermoforming and blow moulding. in: A.I. Isayev (Ed.), Modeling of Polymer Processing, Cart Hanser, Munich 1999, pp. 117–171.
[5] H.G. deLorenzi, H.F. Nied, C.A. Taylor, A numerical/experimental approach to software development for thermoforming simulationism, J. Pressure Vessel Technol. (Trans. ASME) 113 (1991) 102–114.
[6] A.L. Eterovic, K.-J. Bathe, A hyperelastic-based large strain elasto-plastic constitutive formulation with combined isotropic–kinematic hardening using the logarithmic stress and stain measures, Int. J. Numer. Math. Eng. 30 (1990) 1099–1114.
[7] I. Hlavacek, J. Rosenberg, A.E. Beagles, J.R. Whiteman, Variational inequality formulation in strain space and finite element solution of an elasto-plastic problem with hardening, Comp. Meth. Appl. Mech. Eng. 94 (1992) 93–112.
[8] M.S. Kuczma, J.R. Whiteman, Variational inequality formulation for flow theory plasticity, Int. J. Eng. Sci. 33 (1995) 1153–1169.
[9] H.F. Nied, S.A. Taylor, H.G. deLorenzi, Three-dimensional finite element simulation of thermoforming, Polym. Eng. Sci. 30 (1990) 1316–1320.

[10] D.R.J. Owen, E. Hinton, Finite Elements in Plasticity, Pineridge, Swansea, 1980.
[11] J.C. Simo, R.L. Taylor, Consistent tangent operators for rate-independent elastoplasticity, Comp. Meth. Appl. Mech. Eng. 48 (1985) 101–118.
[12] M.-H. Vantal, B. Monasse, M. Bellet, Numerical simulation of thermoforming of multi-layer polymer sheets, in: S.-F. Shen, P. Dawson (Eds.), Simulation of Materials Processing: Theory, Methods and Applications, Balkema, Rotterdam, 1995, pp. 1089–1095.
[13] G.G. Weber, A.M. Lush, A. Zavaliangos, L. Anand, An objective time-integration procedure for isotropic rate-independent and rate-dependent elastic–plastic constitutive equations, Int. J. Plasticity 6 (1990) 701–744.
[14] M.K. Warby, J.R. Whiteman, Finite element model of viscoelastic membrane deformation, Comp. Meth. Appl. Mech. Eng. 68 (1988) 33–54.
[15] M.K. Warby, J.R. Whiteman, Taking the trial and error out of thermoformed container design, Plastics and Rubber (July) (1994) 4–7.
[16] O.C. Zienkiewicz, R.L. Taylor, The finite element method, in: Solid Mechanics, Vol. 2, Butterworths/Heinemann, Oxford, 2000.